投稿論文(英文)
PAPERS

J. of Hydrau., Coast. and Environ. Eng. No. 521/II-32, 227-237, 1995. 8

NUMERICAL STUDY OF TURBULENT STRUCTURE OVER STRIP ROUGHNESS IN OPEN CHANNEL FLOW USING A LOW REYNOLDS NUMBER TURBULENCE MODEL

Akihiro TOMINAGA[1], Jian LIU[2] and Masashi NAGAO[3]

[1]Member of JSCE, Dr. of Eng., Assoc. Prof., Dept. of Civil Eng., Nagoya Inst. of Tech.,
(Gokiso-cho, Showa-ku, Nagoya 466, Japan)
[2]M. Eng., Graduate student, Dept. of Civil Eng., Nagoya Inst. of Tech.
[3]Member of JSCE, Ph.D., Prof., Dept. of Civil Eng., Nagoya Inst. of Tech.

Turbulent structure over strip roughness in open channel flow with various roughness spacing is simulated with a modified low Reynolds number k-ε turbulence model. The effect of the free surface is taken into account in the process of the calculation. The turbulence characteristics in response to the roughness spacing is predicted. Comparisons with the experimental data are generally adequate, in which the predictions for velocities are better than those for turbulent shear stresses and resistance coefficient. The values of the turbulent kinetic energy increase apparently in neighbor of the upstream corner of the roughness. The mixing effects of the flow become strong with the decrease of the roughness spacing.

Key Words : *strip roughness, turbulent structure, free surface, resistance coefficient, roughness spacing, low Reynolds number k-ε turbulence model*

1. INTRODUCTION

Some studies on the flow over rough boundaries have been carried out experimentally and analytically using various kind of roughness elements for basic research and practical purposes. Although, to a certain degree, they provide guidelines for the estimation of hydraulic resistance laws of the roughness in the flow, it is very difficult to determine the properties of the flow over rough bed universally owing to the flow being considerably sensitive to the size, shape and arrangement of roughness elements. On occasion when the size of roughness element is larger compared with the water depth, the flow farther from the walls and the water surface are changed greatly, general expression of the law of such flow is more apparently difficult. Hence, the study of the flow in which roughness element is smaller compared with water depth has been made in the present paper. The resistance of the turbulent flow is generally determined by the size of the dissipation rate of turbulent kinetic energy. The dissipation rate stems from unsteadiness in the vicinity of the outer region of the viscous sublayer for the flow in a smooth open channel, however, for the flow over rough bed, its source is the wake flow due to the roughness. The turbulent structure of the flow over rough bed, however, is very similar to the one in a smooth channel in the outer regions except for neighboring regions of roughness elements[1]. Even though the mechanism of the production of the turbulent kinetic energy is different, it exists in universality of the cascade process of turbulence from the inertial subregion to the viscous dissipation subregion. Hence, the similarity of the turbulent structure normalized by the representing scale of dissipation rate is expected to exist between the flow over rough boundary and the one in smooth boundary. Moreover, it is necessary to understand the mechanism determining the absolute scale of dissipation rate. Generally, the height of roughness element is considered to be a definite factor for the absolute scale, but, the spacing between roughness elements has important influence on resistance coefficient in the flow over strip roughness. With the idea of Adachi[2] and Knight, et al.[3], the hydraulic resistance of roughness attains maximum when the relative spacing L/k defined as the ratio of the spacing L between the roughness elements and the roughness height k is from 6 to 10. If the relative spacing is smaller than 6, there is a dead water region between the roughness elements, and the height responded by the flow is smaller than the actual one; on the other hand, when the spacing of

strip roughness is very large, it is easy to understand that resistance is smaller, since the quantity of roughness elements is small in the total flow area. In the case of the ordinary spacing of the strip roughness, the spacing has some influence on the developing process of the wake flow behind the strip roughness. To discuss the turbulent structure of the flow over two-dimensional strip roughness whose spacing is varied is one of the most basic approach to understand the generation mechanism of turbulent kinetic energy over rough boundary. Many experiments have been made for the flow over strip roughness (See Perry, et al.[4], Futuya, et al.[5] and Antonia, et al.[6]). The experimental results show that the hydraulic resistance of strip roughness is characterized by the relative spacing L/k. According to various patterns of the interaction between the main flow and the wake flow due to the roughness, Perry, et al. classified strip roughness into two categories: the d-type for L/k<4 and the k-type for L/k>4. The patterns of the turbulent flow are apparently different from each other in the two types of roughness. Antonia, et al.[6] and Wood, et al.[7] investigated the turbulent structure in the boundary layer over a k-type roughness and over a d-type roughness, respectively. Recently, Tominaga, et al.[8],[9] conducted measurement on turbulence in open channel flows over circular and rectangular strip roughness, using two-component laser-Doppler anemometer (LDA), respectively. The relative spacing is widely changed to cover many roughness conditions. They found that mean velocity profiles agree with the log-law involving the roughness function; the defect of the mean velocity become largest at the relative spacing L/k=8.

Although a number of detailed experimental studies of the flow over strip roughness have been made, few has been accomplished numerically. In order to find out the flow characteristics fully, the flow over strip roughness in open channel is studied by means of numerical simulation in the present paper, based on basic equations of fluid motion. Use of wall function (WF) as boundary conditions, when solving turbulent flows using the k-ε model, has been relatively successful where property is constant. But for large and irregular property variations in the viscous sublayer and buffer layers, the use of WF presents a fundamental problem[10]. In an attempt to obtain a more general model for prediction of the turbulent flow over strip roughness, the low Reynolds number (LRN) k-ε model will be considered. Unlike the WF approach, a LRN closure attempts to model the turbulent transport across the entire near-wall region. This is especially important for predicting turbulent structure in the neighbor of strip roughness.

Since Jones and Launder[11] were the first to propose a LRN k-ε model for near-turbulence, a number of similar k-ε models were developed in succession to raise the accuracy of prediction. Nezu et al.[12] modified some coefficients in the model of Jones and Launder, in an attempt to improve the performance of the model. In the present paper, the modified LRN turbulence model by Nezu et al.[12] is used to predict the turbulent flow over strip roughness in open channel. The calculated results are compared with the experimental data of Tominaga[9] to check the validity of the modified LRN k-ε model for predicting the turbulent flow over strip roughness in open channel.

2. MATHEMATICAL MODEL

(1) Mean transport equations and turbulence model

The two-dimensional turbulent flow over strip roughness in open channel is described by the Reynolds equations. The variables in the turbulent flow are modeled by a control volume method. The x and y coordinates are chosen in the streamwise direction and the direction normal to the wall, respectively. The turbulence model is based on the LRN k-ε model of Jones and Launder, with some constants modified by Launder et al.[13] and Nezu et al.[12]. The set of elliptic partial differential equations governing mass, momentum, and energy conservation for a steady incompressible flow can be written as follows:

$$\frac{\partial}{\partial x}(u\phi)+\frac{\partial}{\partial y}(v\phi)=\frac{\partial}{\partial x}\left(\Gamma_\phi\frac{\partial\phi}{\partial x}\right)+\frac{\partial}{\partial y}\left(\Gamma_\phi\frac{\partial\phi}{\partial y}\right)+S_\phi \quad (1)$$

where ϕ represents different dependent variables (u, v, k and ε), Γ_ϕ stands for generalized diffusion coefficients, S_ϕ is source terms.

The governing equations for the flow are represented in **Table 1**. The effective viscosity ν_{eff} is the sum of the molecular and turbulent contributions, that is

$$\nu_{eff}=\nu+\nu_t \quad (2)$$

where ν is the kinematic viscosity. ν_t is turbulent viscosity, its value is given by

$$\nu_t=f_\mu C_\mu k^2/\varepsilon \quad (3)$$

The functions f_μ, f_1, f_2 and the empirical

Table 1 Conservation equations

Equation	ϕ	Γ_ϕ	S_ϕ
Continuity	1	0	0
x- momentum	u	ν_{eff}	$-\frac{\partial P}{\rho\partial x}+\frac{\partial}{\partial x}\left(\nu_{eff}\frac{\partial u}{\partial x}\right)+\frac{\partial}{\partial y}\left(\nu_{eff}\frac{\partial v}{\partial x}\right)$
y- momentum	v	ν_{eff}	$-\frac{\partial P}{\rho\partial y}+\frac{\partial}{\partial x}\left(\nu_{eff}\frac{\partial u}{\partial y}\right)+\frac{\partial}{\partial y}\left(\nu_{eff}\frac{\partial v}{\partial y}\right)$
Turbulent kinetic energy k	k	$\nu+\nu_t/\sigma_k$	$P_k-\varepsilon+D$
Turbulent dissipation rate ε	ε	$\nu+\nu_t/\sigma_\varepsilon$	$f_1C_{\varepsilon1}P_k\varepsilon/k-f_2C_{\varepsilon2}\varepsilon^2/k+E$

$$P_k=\nu_t\left[2\left(\frac{\partial u}{\partial x}\right)^2+2\left(\frac{\partial v}{\partial y}\right)^2+\left(\frac{\partial u}{\partial y}+\frac{\partial v}{\partial x}\right)^2\right],\quad D=-C_3\nu\left[\left(\frac{\partial k^{1/2}}{\partial x}\right)^2+\left(\frac{\partial k^{1/2}}{\partial y}\right)^2\right]$$

$$E=C_4\nu\nu_t\left[\left(\frac{\partial^2 u}{\partial x^2}\right)^2+\left(\frac{\partial^2 u}{\partial y^2}\right)^2+\left(\frac{\partial^2 v}{\partial x^2}\right)^2+\left(\frac{\partial^2 v}{\partial y^2}\right)^2\right]$$

coefficients C_μ, $C_{\varepsilon1}$, $C_{\varepsilon2}$, σ_k, σ_ε obtained by Launder and Sharma[13] are adopted:

$$C_\mu=0.09,\ C_{\varepsilon1}=1.44,\ C_{\varepsilon2}=1.92,\ \sigma_k=1.0,\ \sigma_\varepsilon=1.3$$

$$f_1=1.0,\quad f_2=1.0-0.3\exp(-Re_t^2)$$

$$f_\mu=\exp\left[\frac{-3.4}{(1+Re_t/50)^2}\right] \tag{4}$$

where $Re_t=k^2/\nu\varepsilon$ is the turbulent Reynolds number.

In **Table 1**, P_k represents the production of kinetic energy by the interaction of mean velocity gradients and turbulent stresses. Only for the computational reason, the extra term D and generation term E are added to the transport equations of k and ε, respectively. The empirical coefficients C_3 and C_4 in the expression of D and E are proposed to be equal to 2 by Jones and Launder[11]. Nezu et al.[12] modified the value of C_3 based on a number of experimental data, and advocated that $C_3=1.8$ is most suitable for the turbulent flow in open channel. The modified value of C_3 of Nezu et al. is therefore adopted in the present study.

(2) Boundary conditions

Because Eq.(1) is elliptic, it is necessary to define the boundary conditions for all variables on all boundaries of the flow domain, i.e. inlet, exit, solid wall and free surface of flow. At the inlet, the variables can be taken from measurements or log-law profiles, while zero gradients can be set at the outlet. At the surface, however, an attention must be paid to the effects of water surface. It is necessary to modify zero gradients at water surface. Nezu et al.[12] and Handler et al.[14] measured in detail the turbulence characteristic near free surface. In Ref. 12, Nezu et al. introduced a dumping coefficient, D_W, in consideration of the damping effects of kinetic energy at water surface, and recommended that $D_W=0.8$ is suitable for open-channel flows. For the dissipation rate near free surface, although Handler et al. made detailed explication by direct numerical simulation, they yielded no clear conclusions. The boundary condition of dissipation rate near free surface is thus adopted zero gradient in the present study. Because the low Reynolds number approach enables an extension of the k-ε turbulence model all the way to the wall, special treatment near the solid wall is unnecessary.

The regions which locate in the roughness elements are treated by means of the method proposed by Patankar[15], in which the velocity terms are modified. In Ref.15, assigning a desired value of the general variable ϕ to an internal grid point, the linearized source terms Sc and Sp for that point are set, such that

$$Sc=10^{30}\phi_{p,desired}$$

$$Sp=-10^{30} \tag{5}$$

This method works well if ϕ_p desired is not very small. However, when the general variable ϕ stands for velocity u or v and the desired value is zero at internal grid point, the method can't guarantee that the value is equal to zero and often causes divergence

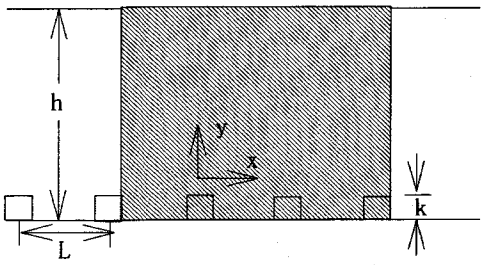

Fig.1 Definition of computation area

of the iteration solution. Hence, the velocities u and v at internal grid point are set to be zero herein for convergence of the iterative solution.

Fully developed flow in a single module is solved by using the periodicity conditions, as proposed by Patankar et al.[16]. The approach of Patankar et al. however requires additional source terms in the momentum and energy equations. The simpler approach to the periodic boundary condition proposed by Chang et al.[10] is therefore used in the present study. A fixed number of inner iterations are performed for given inlet conditions, and the calculated outlet values of velocities, kinetic energy and dissipation rate are substituted as inlet conditions to the next outer iteration. A log-law profile is given for the streamwise velocity at the inlet as the first outer iteration. The computational area shown in **Fig.1** is chosen such that the inlet and the outlet are located at the right end of the roughness elements. The calculated ranges in streamwise direction for different relative spacing L/k are about 35-40 times of water depth, where the flow is fully developed.

(3) Discretization and calculated procedure

The spatial derivatives in Eq.(1) are discretized with the finite-volume method on the staggered grid system proposed by Patankar et al.[15]. The hybrid scheme is used to discretize the convection term. This implies that the second-order accurate central scheme for the convection is locally replaced by the first-order accurate upwind scheme as soon as the grid size exceeds a critical value. In comparison with the use of the central scheme for all grid points, the hybrid scheme is more stable during the iteration process to solve the discretized system.

The profile of the boundary layer requires a non-equidistant grid system along the walls. The sides of the finite volumes near the solid walls are positioned in y direction and in the front and back of roughness according to geometrical progression, and 67% of grids located between the wall and the level of two times of roughness height in y-direction. For low Reynolds number turbulence model, it is usually

Table 2 Hydraulic condition for numerical calculation

	Case	Relative spacing L/k	Relative depth h/k	Mean velocity (cm/s)	Reynolds number Re	Froude number Fr
R1	Ra03	16	16	27.3	2.3×10^4	0.31
	Ra06	8	16	26.4	2.2×10^4	0.30
	Ra09	4	16	26.8	2.2×10^4	0.30
	Ra12	2	16	27.3	2.1×10^4	0.31
R2	Ra04	16	10	23.8	1.4×10^4	0.33
	Ra07	8	10	23.2	1.3×10^4	0.32
	Ra10	4	10	28.7	1.610^4	0.39
	Ra13	2	10	28.1	1.5×10^4	0.39
	Ra15	∞	16	28.7	2.3×10^4	0.32
	Ra16	∞	16	20.9	1.7×10^4	0.24

adequate to place the first node adjacent to the wall somewhere in the viscous sublayer (dimensionless wall distance $y^+<5$), typically $y^+=1$. The first node is placed at $y^+=0.3$-0.5 to decrease the effect of instabilities due to grid in the present paper. The pressure field is calculated by using the SIMPLE method of Patankar et al.[17]. The discretized equations is solved by a tridiagonal matrix algorithm (TDMA). Some under-relaxation is required to prevent divergence of the iteration process.

The criterion of convergence of numerical solution is based on the absolute normalized residents of the equations that is summed for all control volumes in the computation. The solutions are regarded as converged when these normalized residuals become less than 10^{-6} for all variables.

3. PRESENTATION AND DISCUSSION

The various cases shown in **Table 2** are numerically simulated by using the modified low Reynolds number turbulence model. In **Table 2**, the roughness elements are square with cross section of k×k=0.5cm×0.5cm. Relative spacing L/k is changed from 2,4,8,16 up to infinity which means that only one roughness element exists in the flow. Relative flow depth h/k (h is the flow depth measured from the bed) is set to be about 10 and 16, respectively. The Reynolds number Re ($\equiv U_m h/\nu$, U_m is the mean bulk velocity) and the Froude number Fr ($\equiv U_m/\sqrt{gh}$, g is the gravitational acceleration) are separately set to be about $Re=2.2\times10^4$, Fr=0.3 for Group R1 and $Re=1.4\times10^4$, Fr=0.35 for Group R2.

Without specific notification in this section, the predicted and measured values are non-dimensional. The predicted values are the calculated results when outer iterations are equal to 20 for the case of

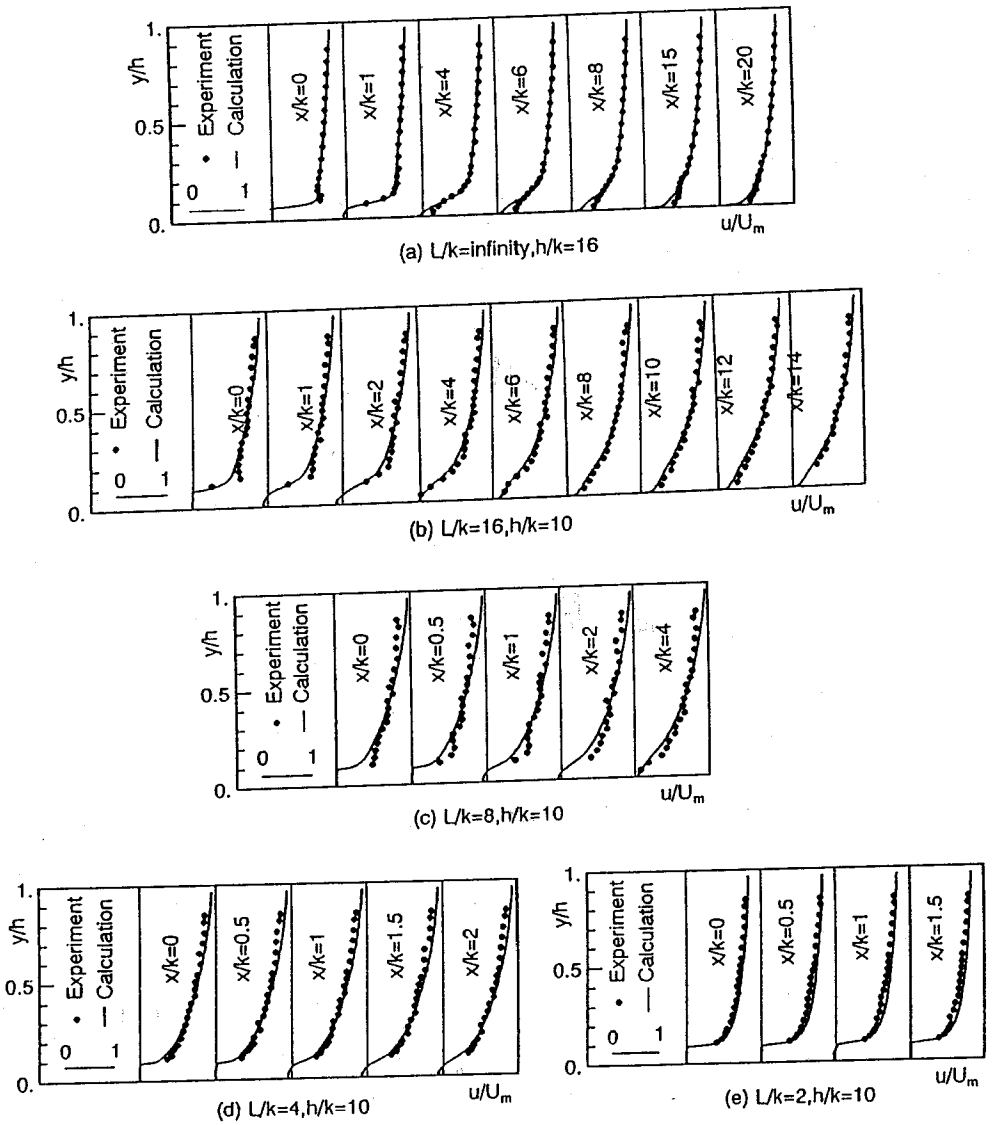

(1) Velocities

Fig. 2 Comparisons of the calculated velocities and Reynolds stresses with the experimental data for Ra15 and Group R2

L/k=16 and 35 for the others except for the case of L/k=∞, respectively. The calculated results are compared with the experimental data of Tominaga[9].

The streamwise velocity and the Reynolds stress distributions based on the calculated values and experimental data of Ra15 and Group R2 are depicted in **Fig.2** (x/k=0 is at the center of the roughness element). The computed velocities are in good agreement with the measurements. The agreement of the calculated Reynolds stresses with the experimental data is generally good, except for the under-prediction of about 15% for both L/k=16 and L/k=2 in the vicinity of the strip roughness. The distributions of the Reynolds stresses $-\overline{uv}/U_m^2$ vary linearly in the region far from the bed. The values of $-\overline{uv}/U_m^2$ near the bed change rapidly. This illustrates that stronger eddy disturbance occur in the vicinity of the roughness, especially, the variation of $-\overline{uv}/U_m^2$ in y-direction for the case of L/k=∞ is most remarkable. Moreover, with the decrease of L/k, the peaks of $-\overline{uv}/U_m^2$ become smaller and smaller until it reaches the minimum value at the case of L/k=2, which brings about some of the characteristics of smooth bed.

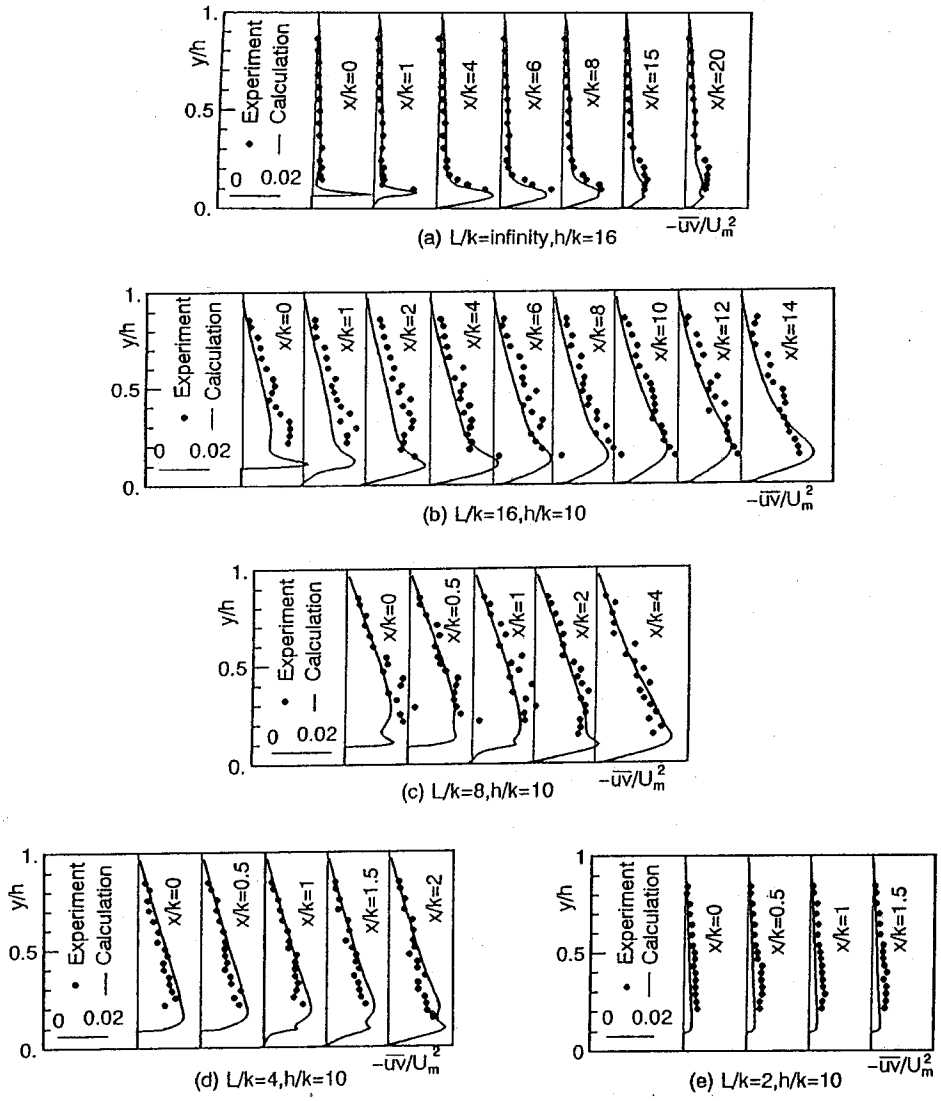

(2) Reynolds stresses

Fig. 2 Continued

Fig.3 shows the comparison of the calculated and measured variations of turbulence intensities u'/U_m for Ra15 and Group R2. Since turbulence kinetic energy k is only calculated in the present model, u' is evaluated approximately so that $u'=0.744\sqrt{2k}$ in the equilibrium region according to Nezu[1]. The calculated turbulence intensities agree well with the experimental data, except for the cases of L/k=2 and L/k=16. The calculated values for the case of L/k=16 are smaller than the experimental values in the region of $y/h \geq 0.7$, and the calculated values for the case of L/k=2 are larger than the experimental values. The errors between the calculated values and experimental data are about 10-15%. This result might be due to the form of the extra term E used in the ε equation[18),19)]. The term is likely to increase the dissipation rate and therefore reduce k in the vicinity of the wall. Thus, the calculated turbulent viscosity would become small, which results in lower peaks of the calculated velocities and Reynolds stresses (see **Fig.2**). It is found that the rapid variations of u'/U_m in y-direction centralize in the region of $y/h<0.2$. This phenomenon also shows that stronger eddy disturbance occur in the vicinity of the wall. The values of u'/U_m in y-direction almost changed linearly in the region $y/h \geq 0.2$.

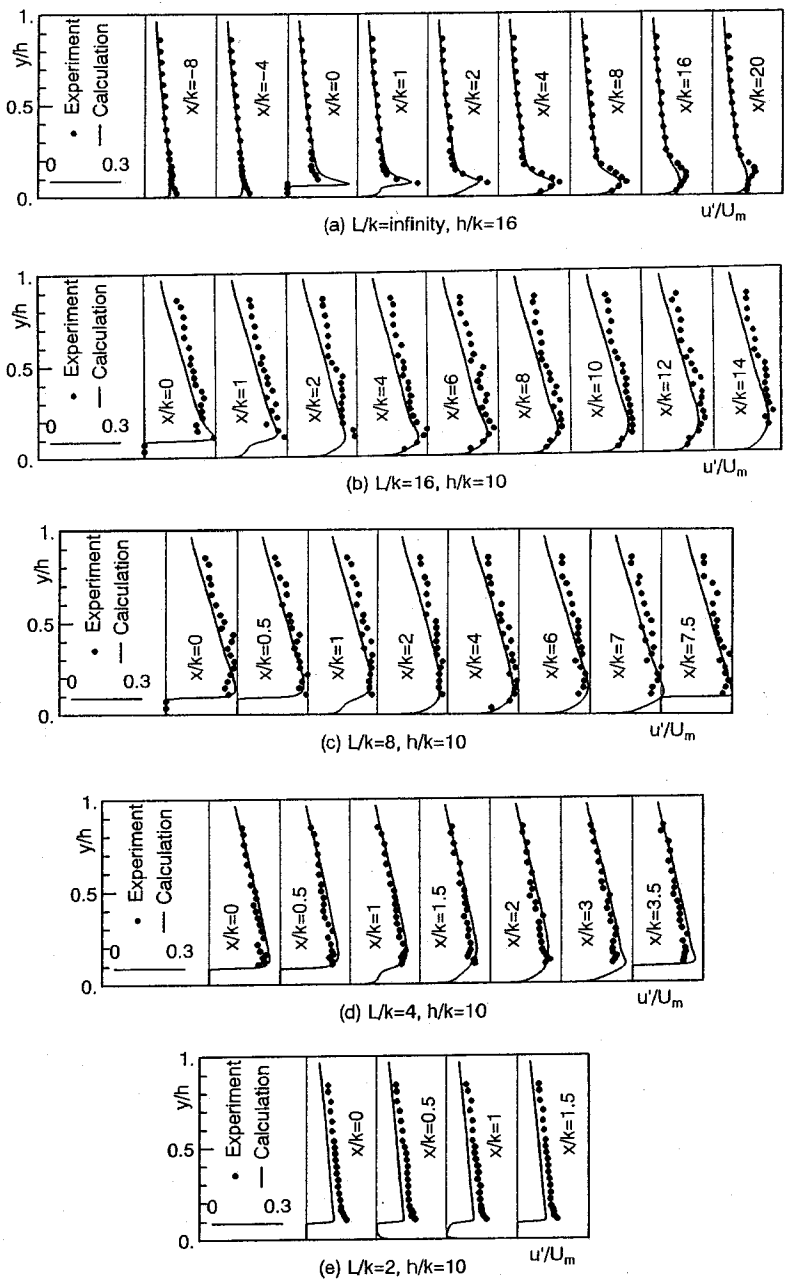

Fig. 3 Calculated and measured turbulence intensities u'/U_m for Ra15 and Group R2

Fig.4 shows the turbulent kinetic energy k/U_m^2 contours of Ra15 and Group R2. Because the computed range is different in one inner iteration, the starting values of the x-coordinates in **Fig.4** are not the same. It is found that the variation of k/U_m^2 in streamwise direction distributes over the region of $y/h<0.2$; the values of k/U_m^2 do not show change in the streamwise direction for $y/h>0.2$. The maximum values of k/U_m^2 occur nearby upstream corners of the roughness where flow impinges, and a highly turbulent shear layer is generated except for the case of L/k=2 (see **Fig.2**), in which the normalized turbulent kinetic energy k/U_m^2 for the case of L/k=8 is the largest among the various cases. Moreover, with the decrease of the relative roughness spacing L/k for the case of $L/k \leq 8$, the values of the turbulent energy k/U_m^2 will decrease rapidly, and no apparent variation in the upstream and the downstream sides of the roughness for the case of L/k=2 is presented; this phenomenon indicates that the dead water

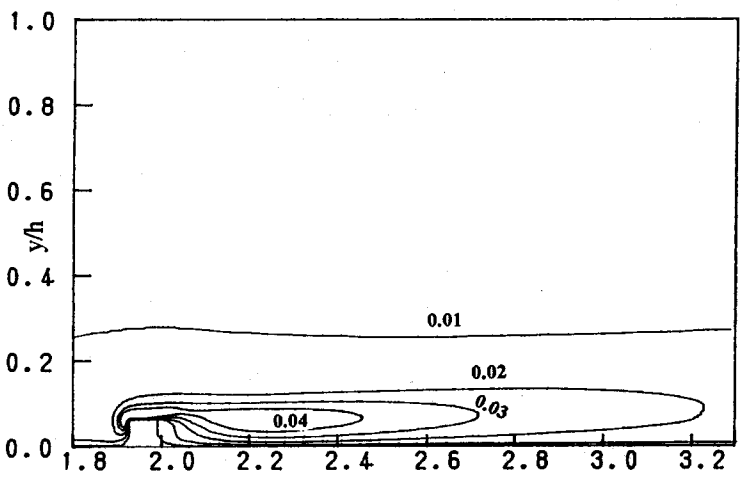

(a) L/k=infinity, h/k=16

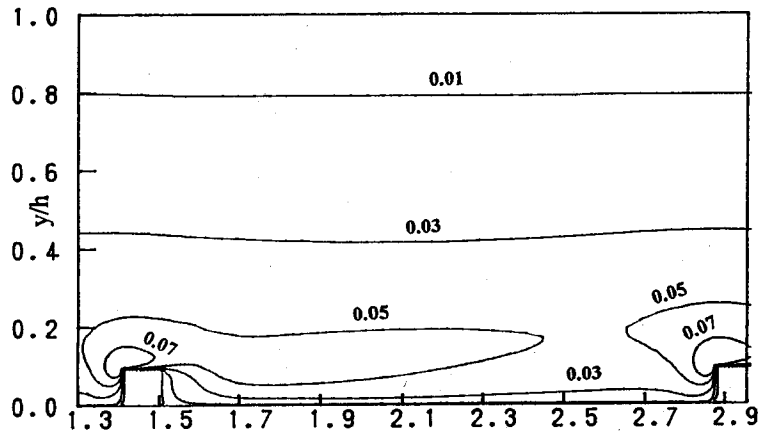

(b) L/k=16, h/k=10

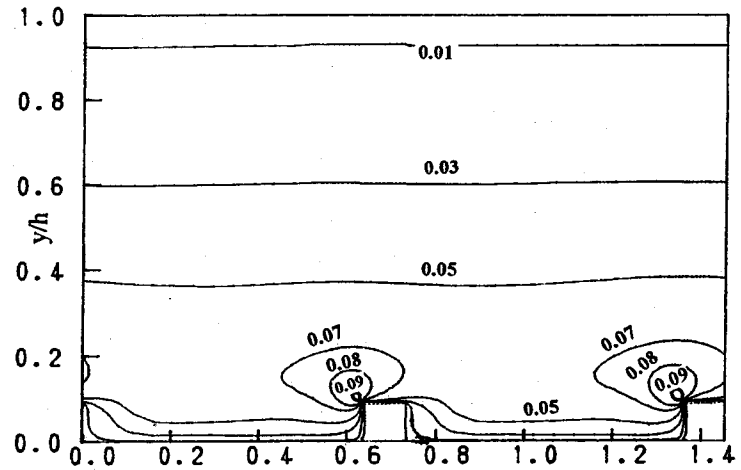

(c) L/k=8, h/k=10

Fig. 4 Turbulent kinetic energy contours for Ra15 and Group R2.

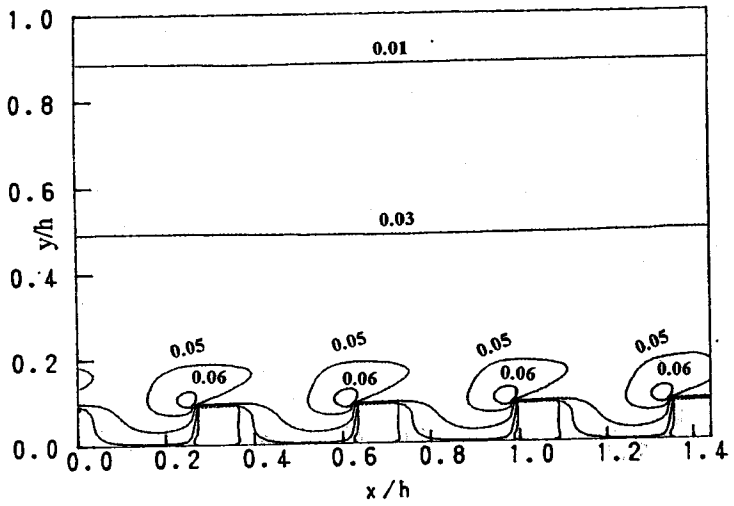

(d) L/k=4, h/k=10

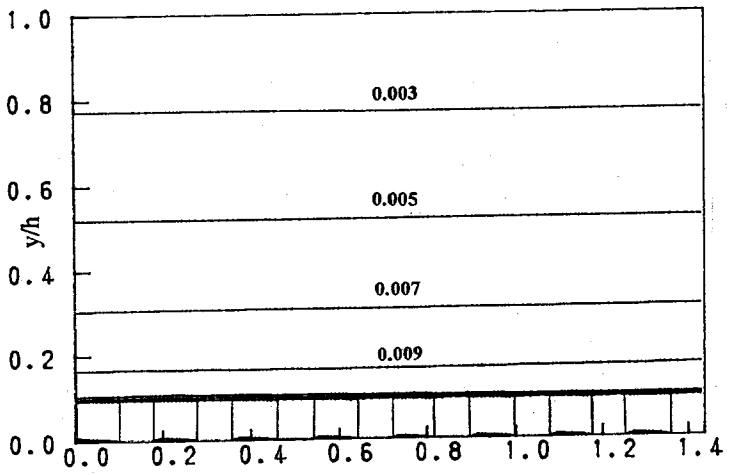

(e) L/k=2, h/k=10

Fig. 4 Continued

basins have been formed between the roughness elements. Because the experimental values of the turbulent kinetic energy in the neighborhood of the roughness elements have not been obtained, the conclusion for case of L/k=2 remains to be tested and verified.

Fig.5 shows the relation between the turbulent production rate P_k and dissipation rate ε ($(P_k-\varepsilon)/\varepsilon$) computed for the case of Ra04. For $0.2 \le y/h \le 0.65$, the dissipation rates are larger than the production rates from x/k=0 (the origin of x coordinate axis is at the center of the roughness element) to x/k=4; the dissipation rates are smaller than the production rates from x/k=6 to x/k=14. For $y/h \ge 0.65$, all dissipation rates are larger than the production rates. It is because of the production rate P_k becoming small owing to the small velocity gradient near to water surface. This phenomenon is almost as same as the one of smooth bed[13].

Fig.6 presents the variation of the vertical distributions of the velocities of Ra15 and Group R1 at the centers of the roughness, as a function of the relative spacing L/k. We can find from **Fig.6** that with the decrease of L/k, the velocities from the roughness to the elevation of y/k=6 will become smaller for the case of $L/k \ge 4$, on the other hand, larger for the case of $L/k \le 4$. The velocity gradient is quite different from each other. The defect of the

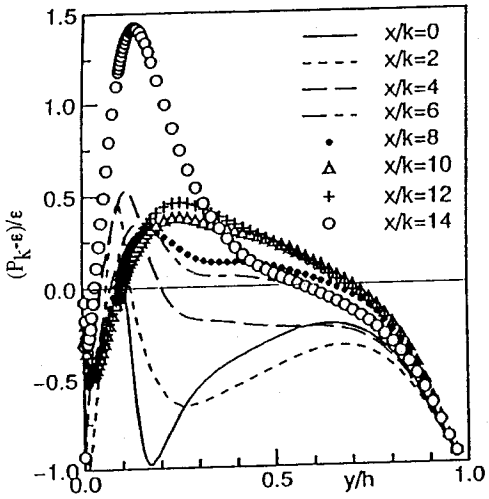

Fig. 5 Calculated relation between turbulence production and dissipation rate for Ra04

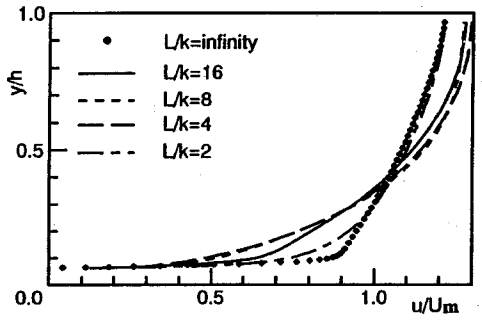

Fig. 6 Variation of vertical distributions of velocities of Ra15 and Group R1 at centers of roughness

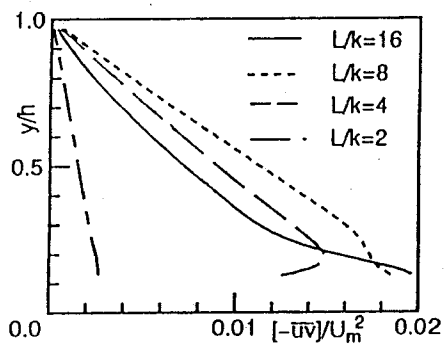

Fig. 7 Distributions of the calculated Reynolds stresses $[-\overline{uv}]/U_m^2$ for Group R2

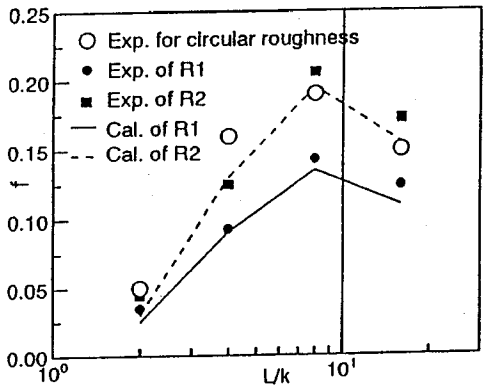

Fig. 8 Comparison of the calculated resistance coefficient with the experimental data

velocity profile becomes smallest in the case of L/k=∞, whereas it becomes largest in the case of L/k=4; this tendency is consistent with the measurements.

Fig.7 shows the distributions of the calculated Reynolds stresses $[-\overline{uv}]/U_m^2$ which are the averaged values between two roughness elements for Group R2. The maximum and the minimum values of $[-\overline{uv}]/U_m^2$ appear at L/k=8 and L/k=2, respectively. This result is identical with the experimental data.

Fig.8 shows a comparison of the resistance coefficient f ($=8(u_*/U_m)^2$, u_* is the friction velocity which is calculated by the Reynolds stress) with the experimental data, together with the previous data obtained by Tominaga and Nezu[8] for the strip roughness with circular cross section of diameter ϕ =8mm, for which the ratio of water depth h to roughness height ϕ is equal to 10. The predicted values are in general good agreement with the experimental data. However, the calculated values for the cases of L/k=2 and L/k=16 are slight smaller than the experimental values. The errors between the calculated values and experimental data are about 15%. This result is mainly due to the calculated Reynolds stresses being smaller than the experimental data. The values of f take peaks at L/k=8. The varying tendency of f for square cross is identical with the one for the circular cross section.

4. CONCLUSIONS

The low-Reynolds turbulence model of Jones and Launder has been successfully modified to be applicable to the turbulent flow over strip roughness in open channel. It has also provided detailed data in close vicinity of the roughness which is not easy to

be experimentally obtained. Prediction for the velocity is better than that for the Reynolds stress, turbulence intensity and resistance coefficient. Further modification to turbulence model is needed to predict the Reynolds stress, turbulence intensity and resistance coefficient better.

From above-mentioned results, with the variation of the roughness spacing, the parameters of the hydraulic characteristics in the vicinity of roughness vary distinctly. The mixing effects of the flow become strong with the decrease of the roughness spacing. The turbulent structure over strip roughness in open channel flow tends gradually to that of smooth flow with the decrease of the relative spacing.

ACKNOWLEDGMENT: The authors are grateful to Professors Nezu, I. and Nakagawa, H. of Kyoto University for providing us with the computer program of the k-ε turbulence model in which free surface effects are considered. The assistance of Mr. Negishi, K. in some of the measurements and Ms. Zhu, S. of Nagoya University in typing manuscript are also gratefully acknowledged.

REFERENCES

1) Nezu, I. : *Turbulent structure in open-channel flows, Ph.D. Thesis*, Kyoto University, 1977 (in Japanese).
2) Adachi, S. : On the artificial strip roughness, *Bulletin*, No.69, Disaster. Prevention. Research Institute, Kyoto University, pp.2-20,1964.
3) Knight, D.W. and Macdonald, J.A.: Hydraulic resistance of artificial strip roughness, *Journal of the Hydraulics Division, ASCE*, Vol. 105, No., HY6, pp.675-690, 1979.
4) Perry, A.E., Shofield, W.H. and Joubert, P. N.: Rough wall turbulent boundary layers, *J.Fluid Mech.*, Vol.37-2, pp.383-413, 1969.
5) Futuya, Y.: Miyata, M. and Fujita, H.: Turbulent boundary layer and flow resistance on plates roughened by wires, *J. Fluid Eng., ASME*, No.76-FE-6, pp.635-644, 1976.
6) Antonia, R.A. and Luxton, R.E. : The response of a turbulent boundary layer to a step change in surface roughness, *J. Fluid. Mech.*, Vol.48-4, pp.721-761, 1971.
7) Wood, D.H. and Antonia, R. A.: Measurements in a turbulent boundary layer over a d-type surface roughness, *J. Appl. Mech., ASME*, pp.591-597, Sept, 1975.
8) Tominaga, A. and Nezu, I.: Turbulent structure past strip roughness in open channel flows, *24th IAHR Congress*, Madrid, pp.c43-ç50, 1991.
9) Tominaga, A.: Effect of relative spacing of strip roughness on turbulent structure in open channel flows, *Proceedings of Hydraulic Engineering, JSCE*, Vol.36, pp.163-168, 1992 (in Japanese).
10) Chang, B.H. and Mills, A.F.: Turbulent flow in a channel with transverse rib heat transfer augmentation, *Int. J. Heat Mass Transfer*, Vol.36. No.6, pp.1459-1469, 1993.
11) Jones, W.P. and Launder, B.E.: The calculation of low-Reynolds number phenomena with a two-equation model of turbulence, *Int. J. Heat Mass Transfer*, Vol.16, pp.1119-1130, 1972.
12) Nezu, I. and Nakagawa, H.: Numerical calculation of turbulent open-channel flows by using a modified K-ε turbulence model, *Proc. of JSCE*, No.387/II-8, 1987 (in Japanese).
13) Launder, B.E. and Sharma, B.I.: Application of the energy dissipation model of turbulence to the calculation of flow near a spinning disc, *Letters in Heat Mass Transfer*, Vol.1, pp.131-138, 1974.
14) Handler, R. A., Swean, Jr., T. F., Leighton, R.I. and Swearingen, J.D.: Length scales and the energy balance for turbulence near a free surface, *AIAA J.*, Vol.31, No.11, pp.1998-2007, Nov., 1993.
15) Patankar, S.V.: *Numerical Heat Transfer and Fluid Flow*, Hemisphere, Washington, D.C., 1980.
16) Patankar, S.V., Liu, C.H. and Sparrow, E.W.: Fully developed flow and heat transfer in ducts having streamwise-periodic variations of cross-sectional area, *J. Heat Transfer*, Vol.99, pp.180-186, 1977.
17) Patankar, S.V. and Spalding, D.B.: A calculation procedure for heat, mass and momentum transfer in three-dimensional parabolic flows, *Int. J. Heat Mass Transfer*, Vol.15, pp.1787-1806, 1972.
18) Patel, V. C., Rodi, W. and Scheuerer, G.: Turbulence models for near-wall and low Reynolds number flows: a review, *AIAA J.*, Vol. 23, No. 9, pp. 1308-1319, 1985.
19) Rodi, W. and Mansour, N. N.: Low Reynolds number k-ε modelling with the aid of direct simulation data, *J. Fluid Mech.*, Vol. 250, pp. 509-529, 1993.

(Received January 23, 1995)

低レイノルズ数乱流モデルによる桟粗度上の開水路流の数値計算

冨永晃宏・劉　建・長尾正志

種々の粗度間隔を有する桟粗度上の開水路流の乱流構造を自由水面の影響も計算に取り入れた低レイノルズ数k-εモデルを用いて数値計算を行い，粗度間隔に対する乱れ構造の応答を予測した．計算値と実験値の一致はおおむね良好であり，流速分布は乱れせん断応力や抵抗係数よりも良く一致した．乱れ運動エネルギーは桟粗度の上流側の角付近で大きな値を取ることがわかった．また，粗度間隔の減少にしたがい，流れの相互作用が強くなることが示された．